JOURNAL
OF THE AMERICAN CHEMICAL SOCIETY

VOLUME 93, NUMBER 23 NOVEMBER 17, 1971

Physical and Inorganic Chemistry

Bonding and Valence Electron Distributions in Molecules. An X-Ray and Neutron Diffraction Study of the Crystal and Molecular Structure of Tetracyanoethylene Oxide[1]

D. A. Matthews,*[2a] J. Swanson, M. H. Mueller,[2b] and G. D. Stucky

Contribution from the School of Chemical Sciences and Materials Research Laboratory, University of Illinois, Urbana, Illinois 61801, and Argonne National Laboratory, Argonne, Illinois 60439.
Received January 8, 1971

Abstract: The crystal structure of tetracyanoethylene oxide has been determined at room temperature from three-dimensional X-ray and neutron diffraction data measured by counter methods. The compound crystallizes in the space group C_{2h}^5-$P2_1/c$ with cell dimensions $a = 9.718$ (5), $b = 6.141$ (3), $c = 12.162$ (5) Å and $\beta = 110.28$ (2)°. The data were corrected for absorption and anisotropic extinction and refined by full-matrix least-squares techniques to weighted R factors of 0.033 for X-ray and 0.043 for neution data. The molecule packs in such a way that each cyano nitrogen closely approaches the triangle formed by the ring carbon and its two exocyclic carbon substituents. Similar packing in a number of closely related tetracyano compounds is discussed in relation to the observed nonlinearity of the C–C–N fragment. The data are shown to be consistent with an explanation for this bending based on delocalization of electron density into the antibonding π orbital of the cyano group. The thermal motion is analyzed in terms of a rigid body approximation.

The molecular and electronic structure of small strained-ring molecules is of interest owing to the apparent breakdown of the concept of directed valence. The extent of this interest is evidenced by the fact that more than 25 "theoretical" papers have been published during the last 20 years on the electron distribution and bonding in cyclopropane alone. In addition, there has been considerable experimental effort directed toward the unusual physical and chemical properties of compounds containing three-membered rings.[3-5] Recently, electron distributions for cyclopropane and a number of three-membered heteroatom ring systems have been studied by more rigorous theoretical methods.[6,7] The only experimental data with which these results can be compared are the X-ray diffraction studies of *cis*-tricyanocyclopropane[8] and 2,5-dimethyl-7,7-dicyanonorcaradiene.[9]

In *cis*-tricyanocyclopropane some small residual electron density was found outside the internuclear C–C axes when difference Fourier sections were calculated in the plane of the cyclopropane ring. No density was observed inside the ring. The center of the cyclopropane ring lies on a crystallographic special position of threefold symmetry. No mention was made of the number of sets of symmetry-equivalent data recorded, but unless a full hemisphere was collected errors near the center of the ring, which is of special interest, may be

(1) This research was supported by the Advanced Research Projects Agency under Contract No. HC 15-67-C-0221, by the National Science Foundation, and by the donors of the Petroleum Research Fund, administered by the American Chemical Society.

(2) (a) University of Illinois Graduate Fellow, 1967–1969; American Chemical Society–Petroleum Research Fund Graduate Fellow, 1969–1970; (b) Argonne National Laboratory.

(3) A. D. Walsh, *Trans. Faraday Soc.*, **45**, 179 (1949).

(4) W. H. Flygare, A. Narath, and W. D. Gwinn, *J. Chem. Phys.*, **36**, 200 (1962).

(5) R. A. Clark and R. A. Fiato, *J. Amer. Chem. Soc.*, **92**, 4736 (1970).

(6) R. Bonaccorsi, E. Scrocco, and J. Tamasi, *J. Chem. Phys.*, **52**, 5270 (1970).

(7) E. Kochanski and J. M. Lehn, *Theor. Chim. Acta*, **14**, 281 (1969).

(8) A. Hartman and F. L. Hirshfeld, *Acta Crystallogr.*, **20**, 80 (1966).

(9) C. J. Fritchie, Jr., *ibid.*, **20**, 27 (1966).

several times larger than those in other regions. A more serious source of concern is that recent results show that systematic errors, especially in thermal parameters, can be expected for light-atom structures refined with spherical atom scattering factors.[10,11] To the extent that the bias in assuming spherical atoms is compensated for by erroneously large atomic thermal parameters, the charge densities sought in X-ray difference maps will be highly obscured or eliminated and interpretations based on these maps must be made with care.

Fritchie found that the agreement between observed and calculated structure amplitudes in 2,5-dimethyl-7,7-dicyanonorcaradiene was significantly improved if instead of spherical atom scattering factors he used scattering factors calculated from various "bent bond" configurations. The optimum angle of bend was found to be 20 (±10)°. In this work any reflections thought to be suffering from extinction were given zero weights in the least-squares refinement. However, it is these generally low-angle reflections which contain the most information about bond charge densities, since the scattering factors for valence charge distributions fall off more rapidly with increasing scattering angle than those of the core electrons. Furthermore, the approach is indirect since it assumes a certain very restricted model for the cyclopropane ring, namely isolated bent bonds, and then proceeds to show the improved agreement over the spherical atom approximation. There may exist a number of models which would give as good or better agreement than that which was tried, and it is clearly desirable to be able to approach the problem from an unbiased viewpoint involving no preconceived assumptions concerning the spatial distributions of charge density.

This study was initiated in the hope that analysis of accurate X-ray and neutron diffraction data together could provide valuable information on the time-averaged charge density distribution in a light-atom heterocyclic three-membered ring molecule. During the course of this work, Coppens completed similar studies on *s*-triazine[12] and oxalic acid[10] and was able to confirm the usefulness of the technique. In this paper we present the room-temperature crystal structure of tetracyanoethylene oxide (TCEO) as determined by X-ray and neutron diffraction. In the following paper we report an experimental determination of the aspherical electron distribution as revealed by an analysis of this data.

Experimental Section

TCEO was prepared by the method of Linn, Webster, and Benson.[13] The crude product was recrystallized from ethylene dichloride and then sublimed at 50° (10^{-5} mm). Well-formed elongated crystals of any desired length up to 1 cm or more are easily obtained by this method. The colorless crystals are stable indefinitely in the absence of water vapor, but noticeable decomposition in the form of a gradual darkening is evident after several days of exposure to air.

Examination of a number of crystals under a microscope using crossed polarizers showed extinction to occur in the direction of crystal elongation. Suitable crystals were mounted with their long axis (coincident with the *b* axis) parallel to the long dimension of thin-walled glass capillary tubes. Precession and Weissenberg photographs showed systematic absences for reflections $0k0$, $k \neq 2n$ and $h0l$, $l \neq 2n$. These absences uniquely define the space group as C_{2h}^{5}-$P2_1/c$. The lattice parameters and their standard deviations determined as described below are: $a = 9.718$ (5), $b = 6.141$ (3), $c = 12.162$ (5) Å, $\alpha = \gamma = 90.0°$, and $\beta = 110.28$ (2)°. The density of 1.38 g/cm³ was measured by flotation in an aqueous zinc chloride solution and agrees well with a calculated density of 1.40 g/cm³ assuming four molecules per unit cell.

(a) **X-Ray.** A rectangular-shaped crystal with dimensions 0.48 × 0.45 × 0.35 mm was mounted as described above for the X-ray diffraction experiment. A computer-controlled four-circle Picker diffractometer with Mo Kα radiation and a highly oriented graphite monochromator was used for all intensity measurements. Ten high-angle reflections falling between 45 and 55° in 2θ were carefully centered about their $K\alpha_1$ component. The final angular settings of these reflections were used in the least-squares calculation of lattice parameters. Pulse-height discriminator settings for 95% peak acceptance and background rejection were obtained from a pulse-height distribution curve for the Kα component of a typical reflection. The takeoff angle was 2.0°. At this angle a strong reflection gave 80% of its maximum value as a function of takeoff angle. Thin Cu foil attenuators were automatically inserted into the diffracted beam in order to avoid counter saturation whenever the counting rate exceeded 10,000 counts/sec.

The crystallographic *b* axis was offset from the φ axis of the diffractometer by small adjustments in the goniometer arcs in order to eliminate wavelength-independent multiple reflection. Integrated intensities were collected using the θ–2θ scan technique with a scan rate of 1°/min. Ten-second standing counts were made at the beginning and end of the scan for each reflection. The scan range was 1.2° symmetrically disposed about $K\alpha_1$. Two standard peaks were monitored every 50 reflections and showed only random fluctuations for the duration of the data collection. A full sphere of data was obtained to a value for 2θ or 70°. This resulted in a total of 13,467 reflections being recorded of which 3021 were unique. Raw intensities were corrected for background, Lorentz–polarization, and absorption.[14] The polarization correction used for the monochromatic radiation was $(1 + \cos^2 2\theta_m \cos^2 2\theta)/(1 + \cos^2 2\theta_m)$, where θ_m is the Bragg angle for the monochromator crystal. A further discussion as to the appropriateness of this expression will be given later. The calculated absorption coefficient of 1.12 cm^{-1} gave transmission factors which varied from 0.93 to 0.97. Spherical atom scattering factors were taken from the compilation of Hansen, *et al.*[15]

(b) **Neutron.** A large single crystal of TCEO measuring 0.47 × 0.33 × 0.30 cm was mounted on the four-circle automated neutron diffractometer at the CP-5 reactor at Argonne National Laboratory. The crystal was fixed to a vanadium pin and enclosed in a thin-walled vanadium can to protect it from possible hydrolysis on prolonged contact with humidified air. Wavelength-independent simultaneous diffraction was eliminated by offsetting the crystal *b* axis from the φ axis of the diffractometer. Intensity data were collected using a θ–2θ scan mode to a value for 2θ of 75°. The neutron wavelength was 1.052 Å. Each peak was step scanned over 6–7° in 2θ using 0.1° steps. The time at each step was controlled by a monitor count. Two standard peaks were checked every 50 reflections and showed no significant variations during data collection. Two forms of data were collected (hkl, $h\bar{k}l$ and $\bar{h}kl$, $hk\bar{l}$) giving a total of 2329 reflections of which 1120 were unique. The raw intensities were corrected for background, Lorentz, and absorption. In molecular crystals absorption of neutrons is primarily a function of the amount of hydrogen present due to the hydrogen atom's high incoherent cross section for thermal neutrons. In the present case, the absence of hydrogen resulted

(10) P. Coppens, T. M. Sabine, R. G. Delaplane, and J. A. Ibers, *Acta Crystallogr., Sect. B*, **25**, 2451 (1965).

(11) D. A. Matthews and G. D. Stucky, *J. Amer. Chem. Soc.*, **93**, 5954 (1971).

(12) P. Coppens, *Science*, **158**, 1577 (1967).

(13) W. J. Linn, O. W. Webster, and R. E. Benson, *J. Amer. Chem. Soc.*, **87**, 3652 (1965).

(14) In addition to local programs for the IBM 360-75, the following programs, many with local variations, were used in this study: FORDAP Fourier program of A. Zalkin; LINUS least-squares program of P. Coppens and W. C. Hamilton, similar to the Busing–Levy ORFLS program, but modified to include anisotropic extinction; ORFFE error and function program of W. R. Busing and H. A. Levy; ORABS II absorption program of D. J. Weke, W. R. Busing, and H. A. Levy; ORTEP plotting program of C. Johnson; FAME-MAGIC-LINK-SYMPL symbolic addition procedure program of R. Dewar and A. Stone; MEAN PLANE least-squares best plane of M. R. Pippy and F. R. Ahmed; rigid-body analysis program of V. Schomaker and K. N. Trueblood.

(15) H. P. Hansen, F. Herman, J. O. Lea, and S. Skillman, *Acta Crystallogr.*, 17, 1040 (1964).

in a linear absorption coefficient of only 0.02 cm^{-1}. Transmission coefficients in all cases were greater than 0.99, so the error in neglecting absorption effects is negligible. However, the correction was made in order to obtain average path lengths for each reflection so that attenuation due to extinction could be computed. A normal isotopic distribution for C, N, and O was confirmed by a mass spectrum for crystals obtained from the same sublimation batch. Coherent neutron scattering amplitudes were taken from the compilation of Bacon.[16]

Monochromator Polarization Factor. A possible significant source of error in X-ray measurements made with monochromator crystals can arise if the assumed form for the polarization factor does not in fact represent the true degree of mosaicity in the monochromator crystal. The forms of the polarization factors for an ideally mosaic and perfect crystal differ increasingly as the value for $2\theta_m$ is increased. The maximum and minimum differences occur regardless of $2\theta_m$ at $2\theta = 90°$ and $2\theta = 0°$, respectively. For a monochromator setting of $2\theta_m = 11.73°$, the maximum difference is about 0.01. It is seen in this case that the ambiguity accompanying the polarization factor can be eliminated by the choice of a suitably low $2\theta_m$.

Weighting Schemes and the Assignment of Unobserved Reflections

(a) X-Ray. Standard deviations were initially assigned to the structure factors on the basis of modified counting statistics given by

$$\sigma(|F|) = (|F|/2I)[CN + 0.25(TC/TB)^2(B_1 + B_2) + (kI)^2]^{1/2} \quad (1)$$

with $k = 0.05$ and where CN is the total integrated peak count obtained in time TC and B_1 and B_2 are the background counts for a total time TB.[17] Reflections for which the background-corrected intensity I was $\leq 3\sigma'(I)$, where $\sigma'(I) = [CN + (TC/TB)^2(B_1 + B_2)]^{1/2}$, were treated as unobserved and assigned raw intensities of $\sigma'(I)$ with standard deviations of $3I_{min}/\sqrt{45}$, where $I_{min} = 3\sigma'(I)$.[18] An alternative estimate of the standard deviation of $|F|$ is obtained from the distribution of the symmetry-related structure factors about their mean. For all reflections where four equivalent members were collected, this estimate was compared to the average of the individual standard deviations as assigned above. The larger of the two values was chosen and divided by $n^{1/2}$, where n is the number of equivalent members which were observed for that reflection. In the case of one-dimensional reflections where only two equivalent members were recorded, the standard deviations cannot be estimated on the basis of population statistics. A plot was made of $|F|$ *vs.* $\sigma(|F|)$ for all reflections whose estimated standard deviations had been previously assigned. From this plot standard deviations were assigned to the remaining reflections on the basis of the magnitude of their structure factors. A predicted weighted R factor, $R_2 = (\Sigma w|F_o - F_c|^2/wF_o^2)^{1/2}$, can be calculated from the F and $\sigma(|F|)$ values if we use $\sigma(|F|)$ as a measure of $|F_o - F_c|$. The computed value for R_2 of 0.021 indicates good agreement among the equivalent members of the two unique octants. Only the structure factors assigned to be observed were used in the subsequent calculations.

(b) Neutron. The weights were assigned as above except that since only two equivalent members were observed for each reflection no estimate of the standard deviations could be made from comparing symmetry-equivalent reflections. The value for k in eq 1 was 0.02. Only reflections with an observed structure amplitude were used in subsequent calculations. The (100) reflection was given zero weight, since the counter received substantial direct beam radiation.

Other criteria for assignment of unobserved reflections were also explored. Refinements were carried out where the requirement for a structure amplitude to be called observed was that I be greater than $1\sigma'(I)$ and $2\sigma'(I)$, respectively. In all cases the maximum shifts in the final parameters were less than 0.25 combined standard deviations when compared to the results of the refinement carried out with the original weights.

Solution and Refinement

The structure was solved by applying the symbolic addition procedure to the X-ray data set.[19] Six starting symbols were chosen on the basis of their interactions as determined by working through several iterations with the SIGMA2[20] formula by hand. The particular choice of initial symbols was based on the magnitude of the E's for these reflections and the number of SIGMA2 interactions with other reflections of high E. Particular emphasis was placed on early interaction with E's greater than 2.5 so as to maintain maximum probability levels during the first several iterative cycles. The direct method programs of Dewar[14] were then used to phase 110 reflections with E greater than 1.5. The E map with the lowest percentage of contradictions (13%) gave the complete structure in addition to two spurious peaks having peak heights slightly less than those of the carbons.

The least-squares refinement proceeded smoothly. The function minimized was $\Sigma w(F_o - |F|_c)$, where $w = 1/\sigma^2(|F|)$. The unaveraged X-ray data set was refined with anisotropic thermal parameters to a final weighted R factor of $R_2 = 0.041$, where $R_2 = (\Sigma w|F_o - F_c|^2/\Sigma wF^2)^{1/2}$. The X-ray thermal parameters were decreased slightly and used with the X-ray positional parameters as starting values for the unaveraged neutron data. After several cycles of least squares, the neutron structure converged to a weighted R factor of 0.091.

Extinction. An examination of the agreement between observed and calculated structure amplitudes revealed that in both data sets the strongest reflections were systematically attenuated, suggesting that extinction was affecting a substantial number of the measured structure factors. In the past, such reflections have often been given zero weight in the structure refinement. However, in accurate structure analysis this is unacceptable, both because in neutron diffraction experiments extinction can be significant for an appreciable fraction of the data and because thermal parameters are systematically shifted whenever extinction-affected data are removed or improperly corrected.[21]

In applying the extinction correction, we have used the recently formulated anisotropic approximation due to Coppens and Hamilton[21] which is a generalization

(16) G. E. Bacon, "Neutron Diffraction," Oxford University Press, London, 1955, p 28.
(17) P. W. R. Corfield, R. J. Doedens, and J. A. Ibers, *Inorg. Chem.*, 6, 197 (1967).
(18) W. C. Hamilton, *Acta Crystallogr.*, 8, 185 (1955).
(19) J. Karle and I. L. Karle, *ibid.*, 21, 849 (1966).
(20) H. Hauptman and J. Karle, "Solution of the Phase Problem. I. The Centrosymmetric Crystal," American Crystallographic Association Monograph, No. 3, The Letter Shop, Wilmington, Del., 1953.
(21) P. Coppens and W. C. Hamilton, *Acta Crystallogr., Sect. A*, 26, 71 (1970).

of the original theory as developed by Zachariasen.[22] In this approximation the mosaic spread for a type I crystal is described by a three-dimensional Gaussian distribution characterized by a tensor **W** and the mean particle domain for a type II crystal is generalized from a sphere to an ellipsoid characterized by a tensor **Z**.

Refinement of the overall scale factor, positional parameters, anisotropic thermal parameters, and isotropic extinction parameter confirmed that in both the X-ray and neutron data sets strong reflections and a number of intermediate strength reflections suffered appreciable extinction. For these refinements, the full data sets before averaging were used. From the expression for the extinction factor y[22] it is apparent that if symmetry-related reflections have unequal average path lengths through the crystal then this factor will be different for these reflections. An additional directional effect is present when extinction is refined anisotropically, since the probability distribution functions for type I and type II crystals need not conform to the symmetry of the space group. Four cycles of isotropic extinction refinement yielded values of 0.035 and 0.062 for R_2 for the X-ray and neutron data, respectively. The isotropic g for the neutron structure was then converted to the six components of the tensor describing the anisotropic mosaic spread, and these elements along with the scale factor, anisotropic thermal parameters, and positional parameters were refined for four cycles yielding a value for R_2 of 0.060. A similar refinement was carried out assuming the type II approximation. The final R_2 factor was 0.060. The positional and thermal parameters for the two refinements differed in all cases by less than one combined standard deviation, so that insofar as the refinement is concerned, it makes no difference which one is used. It is interesting that in several other cases where anisotropic extinction has been considered there is frequently no significant difference between the parameters obtained for the type I and type II approximations. Coppens and Hamilton have argued that in these cases extinction is affected by both particle size and mosaic spread and neither extreme is probably exactly correct.[21] Since the agreement between observed and calculated structure amplitudes was slightly better for the type II refinement, this approximation was used to correct the observed structure factors. Symmetry-related reflections were then averaged to give 828 unique reflections. Three cycles of least squares varying scale factor, positional parameters, and anisotropic thermal parameters gave a final value for R_2 of 0.043. The value for R_1 for all observed reflections was 0.074, where $R_1 = \Sigma||F_o| - |F_c||/\Sigma|F_o|$. For the X-ray structure, several cycles of type I and type II anisotropic extinction resolved a somewhat different anisotropy of mosaic spread and domain size than the neutron structure, and the final value for R_2 dropped to 0.034 in each case. The agreement between observed and calculated structure amplitudes was slightly better for type II extinction, although no positional and thermal parameters differed by more than a combined standard deviation when the results of the two refinements were compared. The decrease in R_2 is significant at the 99.9% confidence level according to the Hamilton ratio test.[23] All observed reflections were increased by the reciprocal of their extinction factor for type II extinction, and the symmetry-related octants averaged to give 1349 unique reflections. Three cycles of least squares on the scale factor and positional and thermal parameters gave a final weighted agreement factor of 0.033. The value for R_1 was 0.043.

Maximum accuracy is obtained by the least-squares method only when the weights assigned to the observations are valid. The requirement is that $w(F_o - F_c)^2$ be a constant function of $|F_o|$ and $\sin\theta/\lambda$.[24] Both weighting schemes are satisfactory according to this criterion. The final estimated standard deviations for an observation of unit weight were 1.65 and 1.59 for the X-ray and neutron structures, respectively.

In Table I we present the final extinction tensors for both X-ray and neutron type I and type II refinements. We may rotate the tensors to a Cartesian reference system and diagonalize them to obtain the eigenvalues and eigenvectors which are also given in Table I. The mosaic spread and mean particle domain size are conveniently illustrated with the standard com-

Table I. Extinction Parameters

X-Ray: Worst Extinction $F_o^2/F_c^2 = 0.81$

Type I

$W_{ij} \times 10^{-4}$

11	22	33	12	13	23
0.21 (6)	0.11 (2)	0.32 (8)	0.01 (2)	−0.18 (4)	0.03 (2)

Principal axes

$\langle\eta_i\rangle$, sec	Direction cosines[a] × 10^3		
19.9	631	−89	−771
15.4	612	669	424
20.5	477	−739	476

Type II

$Z_{ij} \times 10^{-4}$

11	22	33	12	13	23
9.8 (10)	5.2 (8)	6.0 (6)	0.2 (5)	5.1 (7)	2.7 (5)

Principal axes

$\langle r_i\rangle$, μ	Direction cosines × 10^3		
0.16	640	154	752
0.30	−413	894	169
0.70	−647	−419	637

Neutron: Worst Extinction $F_o^2/F_c^2 = 0.55$

Type I

$W_{ij} \times 10^{-4}$

11	22	33	12	13	23
0.30 (7)	0.14 (2)	0.45 (7)	0.01 (2)	0.13 (5)	0.01 (2)

Principal axes

$\langle\eta_i\rangle$, sec	Direction cosines × 10^3		
6.6	458	27	888
14.1	885	72	−460
15.7	−76	997	9

Type II

$Z_{ij} \times 10^{-4}$

11	22	33	12	13	23
9.0 (10)	0.9 (2)	5.2 (6)	−0.9 (3)	−4.8 (6)	0.6 (2)

Principal axes

$\langle r_i\rangle$, μ	Direction cosines × 10^3		
0.34	955	−105	−277
0.61	281	20	960
1.20	−95	−994	49

[a] Direction cosines are relative to the reference axes a, b, c^*.

(22) W. H. Zachariasen, *Acta Crystallogr.*, 23, 558 (1967).
(23) W. C. Hamilton, *ibid.*, 18, 502 (1965).
(24) D. E. Pilling, D. W. Cruickshank, A. Bujosa, F. M. Lovell, and M. R. Truter in "Computing Methods and the Phase Problem in X-ray Crystal Analysis," Pergamon Press, Oxford, 1961, p 45.

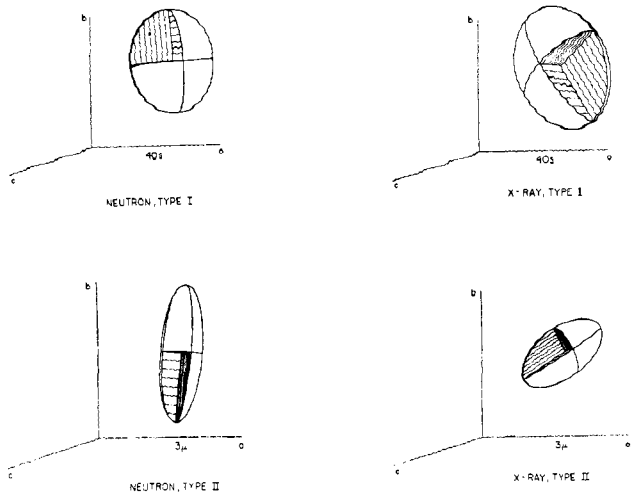

Figure 1. Extinction ellipsoids for TCEO. The principal axes are the rms mosaic spread in seconds for type I extinction and the dimensions of the mean particle domain in microns for type II extinction.

puter programs for drawing thermal vibration ellipsoids.[14] In Figure 1 are illustrated the ellipsoids $\mathbf{X}'\mathbf{W}\mathbf{X} = 1$ and $\mathbf{X}'\mathbf{Z}\mathbf{X} = 1$ for the refinements described above.

The mean particle domain size is seen to be fairly anisotropic in both the neutron and X-ray cases. The crystal used in the neutron experiment has its largest degree of particle perfection along the crystallographic *b* axis, so type II extinction will be most severe for planes which have their normals parallel to the *b* axis. The anisotropy of mosaic spread is slightly less pronounced. According to this interpretation, in the neutron structure the mosaic spread is smallest for planes which have their normals approximately perpendicular to c^*. The results in Table I show that particle domain sizes in both cases are quite small and suggest that any systematic error due to the neglect of primary extinction in the above calculation is probably small. The degree of perfection is seen to be greater for the larger crystal used in the neutron experiment. In this case the particle size varied between 0.34 and 1.2 μ compared with 0.16 and 0.70 μ for the same compound examined using the smaller crystal. A similar result was obtained by Coppens, *et al.*, for α-oxalic acid.[21] The larger crystal was sublimed very slowly over a long period of time. These are conditions which tend to maximize crystal perfection.

The changes in the positional parameters between refinements with and without extinction were typically less than 1.5 times the combined standard deviation. The diagonal elements of the thermal ellipsoid tensors were systematically increased by about 4% in the X-ray case and 10% for the more severely extinction-affected neutron data. These changes represent increases on the order of three combined standard deviations, with some individual values increasing by as many as five combined standard deviations. Clearly, an extinction correction is necessary whenever one of the main purposes of the diffraction study is the determination of accurate thermal parameters. The positional parameters are less sensitive to the systematic error introduced by severe extinction.

Multiple Reflection. The possibility of intensity perturbation due to multiple Bragg scattering was considered in the manner suggested by Coppens.[25] A small number of reflections in both the X-ray and neutron experiments were found to approximately satisfy the equations for multiple scattering. Additional X-ray and neutron data sets were collected at λ 1.541 and 1.575 Å, respectively. It was then possible to calculate a scale factor *c* relating the respective data at different wavelengths and compare this scale factor to the ratio of the intensities for the reflection in question. At the second wavelength the condition for multiple reflection was no longer satisfied, and if this type of error were serious the individual intensity ratios should show systematic deviations from *c*. No disagreement was found and it was concluded that *k*, *k'*, and *k''* (eq 2 in ref 25) were all small for this work, so systematic changes in intensity due to multiple reflection were not significant.

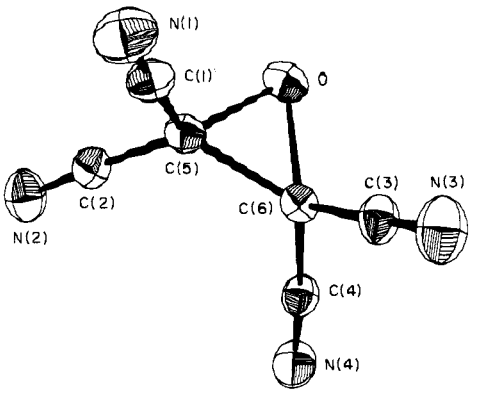

Figure 2. The molecular structure and anisotropic thermal ellipsoids for TCEO. X-Ray and neutron bond distances are given in Table III.

Discussion

Figure 2 shows a drawing of the molecule and indicates the numbering and thermal ellipsoids for the individual atoms. Table II gives the positional and anisotropic thermal parameters for both the neutron and X-ray structures.[26] The differences are seen to be small but often significant, especially for the thermal parameters, and are discussed at length in the following paper. The higher standard deviations for the neutron structure are attributable to the smaller amount of data compared to the X-ray case. The hypothesis that all sets of chemically equivalent but crystallographically independent bond lengths and angles for each structure are equal was tested by analysis of variance techniques. In no case could the hypothesis be rejected at better than the 25% significance level, and for all sets excluding the neutron C–N and C–C distances the significance level for rejection was considerably higher. We therefore report the mean and its standard deviation as well as the individual distances in Table III.

The average neutron bond lengths corrected for rigid-body librations (discussed below) are 1.424 (4), 1.501 (4), 1.453 (3), and 1.140 (2) for the C–O, endo-

(25) P. Coppens, *Acta Crystallogr., Sect. A*, **24**, 253 (1968).

(26) Neutron and X-ray structure factor tables will appear following these pages in the microfilm edition of this volume of the journal. Single copies may be obtained from the Reprint Department, ACS Publications, 1155 Sixteenth St., N.W., Washington, D. C. 20036, by referring to author, title of article, volume, and page number. Remit $3.00 for photocopy or $2.00 for microfiche.

Table II. Fractional Coordinates and Thermal Parameters[a]

	X	Y	Z	β_{11}	β_{22}	β_{33}	β_{12}	β_{13}	β_{23}
O	0.8486 (4)	0.3429 (6)	0.4073 (3)	94 (4)	198 (12)	66 (3)	24 (6)	0 (3)	26 (5)
	0.8489 (1)	0.3408 (1)	0.4072 (1)	110 (1)	242 (3)	75 (1)	18 (1)	10 (1)	24 (1)
C(1)	0.7394 (3)	0.3111 (5)	0.1949 (2)	109 (4)	168 (9)	54 (2)	2 (5)	31 (2)	−27 (4)
	0.7394 (1)	0.3106 (2)	0.1947 (1)	118 (2)	196 (3)	72 (1)	9 (2)	42 (1)	4 (2)
C(2)	0.8756 (3)	0.6413 (6)	0.2847 (3)	79 (3)	209 (11)	86 (3)	−27 (5)	33 (3)	−3 (4)
	0.8761 (1)	0.6425 (2)	0.2850 (1)	96 (2)	234 (4)	91 (1)	−8 (2)	39 (1)	0 (2)
C(3)	0.5829 (3)	0.3261 (6)	0.3540 (2)	97 (4)	189 (10)	61 (2)	−37 (6)	32 (2)	−10 (4)
	0.5827 (1)	0.3265 (2)	0.3536 (1)	117 (2)	215 (3)	60 (1)	−14 (2)	35 (1)	−4 (1)
C(4)	0.7205 (3)	0.6546 (6)	0.4462 (3)	130 (4)	224 (11)	61 (2)	−28 (6)	37 (3)	−39 (5)
	0.7205 (1)	0.6563 (3)	0.4465 (1)	143 (2)	252 (4)	67 (1)	−35 (2)	38 (1)	−21 (2)
C(5)	0.7960 (3)	0.4500 (5)	0.2970 (2)	64 (3)	168 (9)	62 (2)	−6 (4)	22 (2)	−5 (4)
	0.7960 (1)	0.4497 (2)	0.2968 (1)	84 (1)	189 (3)	66 (1)	6 (2)	22 (1)	3 (1)
C(6)	0.7153 (3)	0.4577 (5)	0.3814 (2)	88 (3)	171 (8)	40 (2)	−13 (5)	18 (2)	1 (4)
	0.7147 (1)	0.4571 (2)	0.3811 (1)	100 (2)	198 (3)	55 (1)	−9 (2)	20 (1)	2 (1)
N(1)	0.6913 (3)	0.1999 (5)	0.1168 (2)	194 (4)	262 (9)	69 (2)	−18 (5)	44 (2)	−38 (4)
	0.6911 (1)	0.1980 (3)	0.1171 (1)	206 (2)	290 (4)	87 (1)	5 (2)	49 (1)	−20 (2)
N(2)	0.9378 (3)	0.7951 (5)	0.2789 (3)	136 (4)	272 (9)	156 (3)	−79 (5)	66 (3)	8 (5)
	0.9373 (1)	0.7946 (2)	0.2782 (1)	153 (2)	341 (5)	165 (2)	−48 (2)	71 (1)	12 (2)
N(3)	0.4783 (3)	0.2262 (5)	0.3247 (2)	121 (3)	294 (9)	89 (2)	−75 (5)	38 (2)	−24 (4)
	0.4789 (1)	0.2259 (2)	0.3245 (1)	155 (2)	354 (4)	98 (1)	−66 (3)	50 (1)	−21 (2)
N(4)	0.7285 (4)	0.8170 (6)	0.4946 (3)	268 (6)	272 (11)	109 (3)	−47 (6)	78 (3)	−74 (5)
	0.7284 (2)	0.8162 (2)	0.4939 (1)	271 (2)	329 (5)	120 (1)	−44 (2)	80 (2)	−62 (2)

[a] Neutron values are on the first line. The form of the anisotropic thermal function is $\exp(-\beta_{11}h^2 - \beta_{22}k^2 - \beta_{33}l^2 - 2\beta_{12}hk - 2\beta_{13}hl - 2\beta_{23}kl)$. The values of β are multiplied by 10^4.

Table III. Bond Lengths and Bond Angles for TCEO

Bond	X-Ray	Mean	Neutron	Mean
C(5)–O	1.426 (2)		1.421 (4)	
		1.424 (1)		1.416 (3)
C(6)–O	1.423 (2)		1.411 (4)	
C(3)–C(6)	1.449 (2)		1.456 (4)	
C(4)–C(6)	1.449 (2)		1.435 (5)	
		1.450 (1)		1.446 (2)
C(5)–C(2)	1.451 (2)		1.443 (4)	
C(5)–C(1)	1.449 (2)		1.448 (3)	
C(3)–N(3)	1.130 (2)		1.134 (3)	
C(4)–N(4)	1.128 (3)		1.146 (4)	
		1.129 (1)		1.136 (2)
C(2)–N(2)	1.126 (2)		1.136 (4)	
C(1)–N(1)	1.132 (2)		1.132 (3)	
C(5)–C(6)	1.496 (2)	1.496 (2)	1.493 (3)	1.493 (3)
Angle				
N(2)–C(2)–C(5)	178.1 (14)		177.3 (9)	
N(1)–C(1)–C(5)	176.9 (7)		177.4 (9)	
		176.2 (3)		176.0 (3)
N(4)–C(4)–C(6)	176.5 (6)		176.4 (6)	
N(3)–C(3)–C(6)	175.5 (5)		175.3 (4)	
C(5)–C(6)–O	58.4 (1)		58.5 (2)	
		58.3 (1)		58.2 (1)
C(6)–C(5)–O	58.2 (1)		57.9 (2)	
C(5)–O–C(6)	63.4 (1)	63.4 (1)	63.6 (2)	63.6 (2)
C(1)–C(5)–O	115.9 (2)		116.2 (3)	
C(2)–C(5)–O	116.4 (2)		116.4 (3)	
		116.3 (1)		116.3 (1)
C(3)–C(6)–O	116.3 (2)		116.3 (3)	
C(4)–C(6)–O	116.3 (1)		116.3 (1)	
C(3)–C(6)–C(5)	117.3 (2)		117.2 (2)	
C(4)–C(6)–C(5)	118.2 (2)		118.6 (3)	
		118.0 (1)		118.0 (1)
C(1)–C(5)–C(6)	118.1 (1)		118.3 (2)	
C(2)–C(5)–C(6)	118.1 (1)		118.3 (3)	
C(1)–C(5)–C(2)	116.9 (2)		116.7 (2)	
		117.1 (1)		116.8 (1)
C(3)–C(6)–C(4)	117.2 (2)		116.9 (3)	

Table IV. Selected Intermolecular Distances[a]

	Molecule	Distance
1 C(3)···N(3)	A	3.196 (4)
2 C(5)···N(3)	A	3.072 (4)
3 C(5)···N(2)	B	3.178 (4)
4 C(6)···N(3)	A	3.045 (4)
5 C(1)···N(3)	A	3.268 (4)
6 C(1)···N(2)	B	3.043 (4)
7 N(1)···C(3)	C	3.003 (4)
8 N(1)···C(4)	C	3.087 (4)
9 N(1)···C(6)	C	3.107 (4)
10 C(4)···N(3)	A	3.220 (4)
11 N(4)···C(1)	D	3.314 (4)
12 N(4)···C(2)	D	3.325 (4)
13 N(4)···N(1)	D	3.393 (4)
14 C(2)···N(2)	B	3.062 (4)
15 C(2)···N(3)	A	3.271 (4)

[a] The first atom in each case is at x, y, z corresponding to the parameters in Table I. The distance given is from this atom to the atom in the molecule specified by the letters A–D: (A) $1 - x$, $0.5 + y$, $0.5 - z$; (B) $2 - x$, $-0.5 + y$, $0.5 - z$; (C) x, $0.5 - y$, $-0.5 + z$; (D) x, $1.5 - y$, $0.5 + z$.

cyclic C–C, exocyclic C–C, and C–N distances, respectively. The C–O bond length agrees well with results obtained by microwave spectroscopy for ethylene oxide.[27] The endocyclic C–C distance in TCEO is 0.030 Å larger than that obtained for ethylene oxide, and may reflect a weakening of this bond due to electron withdrawal by the strongly electronegative cyano groups. However, the meanings of measured bond lengths for the diffraction and microwave experiments are different and the significance of small disagreements is difficult to estimate. The endocyclic C–C and C–N distances agree closely with those obtained by Hartman and Hirshfield in their X-ray investigation of *cis*-1,2,3-tricyanocyclopropane.[8] In both cases, however, the thermally corrected C–N distance is distinctly shorter than the expected value of about 1.16 Å.[28] This is probably due to the nonrigorous nature of the rigid-body approximation when applied to molecules containing cyano groups which can undergo a variety of internal low-frequency high-amplitude wags and bends.

(27) G. L. Cunningham, A. W. Boyd, R. J. Myers, W. D. Gwinn, and W. J. LeVan, *J. Chem. Phys.*, 19, 676 (1951).

(28) D. Britton in "Perspectives in Structural Chemistry," Vol. 1, J. D. Dunitz and J. A. Ibers, Ed., Wiley, New York, N. Y., 1967, Chapter 3.

The molecules are packed so that the C(5)–C(6) bond is perpendicular to the *b* axis and the normal to the plane of the ring makes an angle of about 34° with the *b* axis. The $C(CN)_2$ fragments were expected to be planar; however, χ^2 tests on the deviations from the weighted least-squares planes through both groups for both structures showed deviations from planarity at the 0.1% significance level. This is discussed in greater detail below.

The arrangement of molecules in the unit cell is shown in Figure 3. Some of the shorter interatomic distances are given in Table IV. They are all seen to involve at least one nitrogen atom. Three of the four nitrogen atoms make close, approximately equidistant approaches to either the C(1)–C(2)–C(5) or the C(3)–C(4)–C(6) group of adjacent molecules. An examination of a variety of other crystal structures which contain the $C(CN)_2$ group, such as monoclinic tetracyanoethylene (TCE),[29] tetracyanoquinodimethane (TCNQ),[30] and the TCE–anthracene adduct,[31] reveals that close nitrogen approach to this carbon group is a characteristic packing feature of these molecules. Apparently a donor–acceptor interaction exists between the strongly electron-withdrawing cyanide group and the electron-deficient portion of the molecule, *i.e.*, the C(1)–C(2)–C(5) group. It should be pointed out that while this type of packing for the C–C–N group is observed for the above compounds it is not found in cubic TCE,[32] *cis*-tricyanocyclopropane,[8] or tetracyanocyclobutane.[33]

The N(3) atom approaches an adjacent molecule from the side of the three-menbered ring opposite the oxygen atom and closely contacts both C(1)–C(2)–C(5) and C(3)–C(4)–C(6) at an average distance of 3.17 Å. The N(2) and N(1) atoms approach C(1)–C(2)–C(5) and C(3)–C(4)–C(6), respectively, from the C–O side of the three-membered ring at average distances of 3.09 and 3.07 Å. The distances from N(4) to C(1)–C(2)–C(5) are considerably longer. This nitrogen atom has the largest mean-square amplitudes of vibration, while N(3), which has short contacts with both carbon groups, exhibits the most restricted thermal motion.

Table V shows that the carbon–nitrogen bond axis is bent away from the exocyclic C–C bond axis for each of the four crystallographically independent C–C–N fragments. Each nitrogen is on the surface of a right circular cone with principal axis A(2)–A(3) (see Table V) and with a generating angle for the cone of approximately 4°. In order to establish the direction of this bend, we have calculated the signed dihedral angle between the plane defined by the endocyclic and the two exocyclic carbons and the plane of the endocyclic carbon and cyano group. The results for both the neutron and X-ray structures are presented in Table V. It is interesting that in every case the nitrogen is bent away from the cyano group on the same carbon and rotated slightly toward the cyano group on the other ring carbon atom to which it is related by the molecular psuedo-mirror plane.

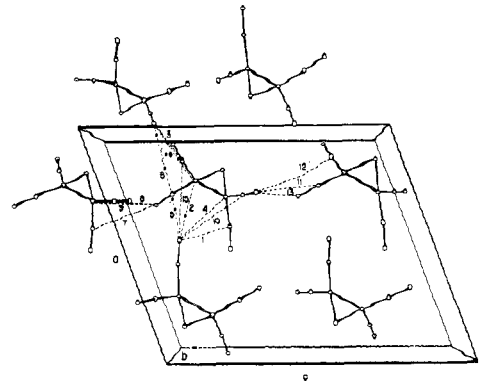

Figure 3. Molecular packing. The numbers identify the distances given in Table IV.

The nonlinearity of the C–C–N group has been noted a number of times before, but often the standard deviations for this angle were such as to preclude any meaningful discussion of the effect. "Packing forces" have sometimes been invoked as an explanation for this nonlinearity,[34] but discussions concerning just what these forces are, how they are directed, and even in what direction the N is shifted off the C–C axis have been conspicuously absent. The other mechanism which has been proposed is based on intramolecular repulsions and predicts a bent bond between the exocyclic and endocyclic carbons.[35] Some of the more precise determinations of this angle were reported for the crystal structures of cubic TCE,[32] *cis*-tricyanocyclopropane,[8] tetracyanocyclobutane,[33] TCNQ,[30] monoclinic TCE,[29] and bis (*tert*-butyl isocyanide)(tetracyanoethylene)nickel(0) (Ni(TCE)(*tert*-BuNC)$_2$).[34] The

Table V. Selected Dihedral Angles[a]

A(1)	A(2)	A(3)	A(4)	Neutrons[b]	X-Rays[b]	ϕ[c]
C(3)	C(6)	C(4)	N(4)	144 (6)	141 (2)	36
C(4)	C(6)	C(3)	N(3)	−177 (4)	−123 (1)	63
C(1)	C(5)	C(2)	N(2)	−164 (7)	−155 (3)	16
C(2)	C(5)	C(1)	N(1)	155 (7)	162 (2)	25

[a] If the two groups of atoms are A(1)–A(2)–A(3) and A(2)–A(3)–A(4), then define the vector $V(1)$ from A(1) to A(2) and $V(2)$ from A(1) to A(3). The plane normal is $V(1)V(2)$. Form a similar normal to the plane of A(2)–A(3)–A(4). The signed dihedral angle is positive for a counterclockwise rotation of the first plane normal into the second when looking from A(2) to A(3)

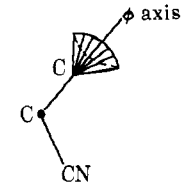

[b] Standard deviations are in parentheses. [c] ϕ is the angle of rotation about A(2)–A(3). When the nitrogen atom assumes a position coplanar with the plane of a ring carbon and its two cyano carbon substituents, but is bent away from the adjacent cyano group on the same endocyclic carbon, ϕ is defined to be zero. Positive values of ϕ rotate the nitrogen in toward the cyano groups on the other ring carbon atom. The values of ϕ are for the neutron structure.

(29) D. A. Bekoe and K. N. Trueblood, *Z. Kristallogr., Kristallgeometrie, Kristallphys., Kristallchem.*, 113, 1 (1960).
(30) R. E. Long, R. A. Sparks, and K. N. Trueblood, *Acta Crystallogr.*, 18, 932 (1965).
(31) I. Karle and A. V. Fratini, *ibid., Sect. B*, 26, 596 (1970).
(32) P. Coppens, private communication.
(33) B. Greenberg and B. Post, *Acta Crystallogr., Sect. B*, 24, 918 (1968).
(34) J. K. Stalick and J. A. Ibers, *J. Amer. Chem. Soc.*, 92, 5333 (1970).
(35) F. L. Hirshfeld, *Isr. J. Chem.*, 2, 87 (1964).

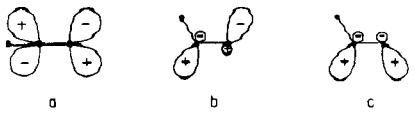

Figure 4. (a) Antibonding cyano π orbital. (b) Trans bent state for the C–C–N fragment; sp^2 atomic orbitals, constituting nearly nonbonding molecular orbitals. (c) Cis bent state for the C–C–N fragment, sp^2 atomic orbitals constituting nearly nonbonding molecular orbitals.

first three are known to contain C–C–N fragments bent in varying degrees, but are not discussed further here since the molecular packing about the C–C–N group is entirely dissimilar to that found in monoclinic TCE, TCEO, and TCNQ. Therefore, the intermolecular forces may be quite different. Some angles and intramolecular nonbonded distances which will be helpful in considering the origin of this effect in TCEO are given in Table VI.

Table VI. Intramolecular Nonbonded Distances and C–C–N Angles[a]

Distances	Monoclinic TCE	Ni(TCE)-(*tert*-BuNC)$_2$	TCEO (X-ray)	TCNQ
C(3)···C(1)	2.814	2.865 (7)	2.847 (2)	
C(2)···C(4)	2.814	2.817 (7)	2.866 (2)	
C(3)···C(4)	2.467	2.430	2.474 (2)	2.434
C(1)···C(2)	2.467	2.406	2.472 (2)	2.434
N(3)···N(4)	4.396	4.385	4.450 (3)	4.381
N(1)···N(2)	4.396	4.301	4.442 (2)	4.381
N(3)···N(1)	3.989	3.989	3.776 (2)	
N(2)···N(4)	3.989	3.847	3.836 (2)	
Ni···C(1)		2.854 (5)		
Ni···C(2)		2.873 (5)		
Ni···C(3)		2.902 (5)		
Ni···C(4)		2.839 (5)		
Angle				
C(5)–C(1)–N(1)	179.6 (5)	178.4 (6)	177.0 (6)	179.4 (2)
C(5)–C(2)–N(2)	179.8 (5)	179.4 (5)	178.2 (14)	179.6 (2)
C(6)–C(3)–N(3)	179.8 (5)	179.7 (5)	175.5 (4)	179.6 (2)
C(6)–C(4)–N(4)	179.6 (5)	177.3 (4)	176.5 (4)	179.4 (2)

[a] Estimated standard deviations are given only when reported in the original paper.

As discussed previously, the packing around the cyano groups in TCE and TCEO is almost identical. Reference to Table VI shows that all four C–C–N groups are linear in monoclinic TCE, but are significantly bent in TCEO. In TCNQ, the same packing alluded to above occurs around one of the two cyano groups; however, the other crystallographically independent group has a distinctly different environment but there is no apparent bend for either of the C–C–N fragments. These data indicate that while the role of intermolecular forces may have some effect on this angle in these compounds, it is not the only contributing factor.

Hirshfeld has reported a nonlinear C–C–N fragment in *cis*-tricyanocyclopropane.[8] He attributes this to a bending of the exocyclic–endocyclic C–C bond with a subsequent rotation of the exocyclic valence orbital as a result of carbon–hydrogen repulsion. The observed bending is consistent with this view. Applying this argument to TCE and its derivatives, we would expect this bend to be more severe for TCNQ, TCE, and Ni(TCE)(*tert*-BuNC)$_2$ than for TCEO, since the former group is characterized by significantly shorter C(1)–C(2) and C(3)–C(4) intramolecular contacts (Table VI). In fact, the opposite is observed and it seems that this argument is not applicable to TCEO.

We now propose an explanation of our results based on a delocalization of lone-pair electron density from the oxygen into the antibonding π orbitals of the cyano group. In our discussions, we assume that all lone-pair electrons on nitrogen are well localized because of their high 2s character. The atomic orbitals to be used as a basis for the treatment are thus the two $2p\pi$ orbitals on each nitrogen and exocyclic carbon and the two lone-pair orbitals on the oxygen. Using the π orbitals as a basis for the generation of a reducible representation in point group C_{2v}, we find, in addition to others, a symmetry orbital of A_1 symmetry which can be visualized as a linear combination of the antibonding π cyano group orbitals. This orbital combines with a lone-pair symmetry orbital of A_1 symmetry on the oxygen to produce a molecular orbital of the same symmetry. The degree of π^* character in this molecular orbital could be established by, for example, an SCF calculation, but such calculations on molecules of this size are difficult and expensive. In the absence of such evidence, we assume some small delocalization of the lone-pair density into the π^* cyano orbitals on the basis of correct symmetry and favorable overlap (oxygen to exocyclic carbon is 2.43 Å).

Figure 4a represents an antibonding π orbital for one of the cyano groups. Evidently, there will be much electrostatic repulsion between any electrons occupying this orbital and electrons in the C–C bond and nitrogen lone-pair orbital. If the linear sp hybridization which determines the σ-bond framework of the cyano group were to change from sp to sp^2 the bond angle of C–C–N would change from 180 toward 120° and in a first approximation we would have two sp^2 hybrid orbitals each capable of holding a pair of electrons. This situation is represented in Figures 4b and 4c for the two possible bends. A similar argument has been used by Ingold and King to postulate a bent configuration for the π^* excited state of acetylene.[36] They point out that the sp^2 atomic orbitals will interact so that electrons entering them will not be completely nonbonding. In TCEO we are talking about a very small quantitative change in hybridization. The angle will probably be more sensitive to the slight change in hybridization than the C–N bond length.

In Ni(TCE)(*tert*-BuNC)$_2$, the local symmetry about TCE is almost C_{2v}. Ni atomic orbitals containing some of the 3d electrons and the 4s atomic orbital transform as a_{1g} and will mix with ligand group orbitals of the same symmetry. To the extent that the cyano π^* orbitals contribute to this molecular orbital, we expect slight nonlinearity of the C–C–N fragment due to delocalization arguments similar to the above. The molecular packing in Ni(TCE)(*tert*-BuNC)$_2$ is not the same as that in TCE, TCEO, and TCNQ so that quantitative comparisons are difficult. However, we can note the following. Shorter nickel–exocyclic carbon distances should permit more favorable nickel orbital–π^* cyano orbital overlap and accordingly more bend in the C–C–N fragment. This expectation is fulfilled without ex-

(36) C. K. Ingold and G. W. King, *J. Chem. Soc.*, 2702 (1953).

ception, as can be seen by a comparison of the relevant distances and angles in Table VI. TCE and TCNQ do not possess any suitable lone-pair or "back-bonding" electrons and should not exhibit nonlinear C–C–N groups resulting from this mechanism.

The neutron anisotropic thermal parameters for all 11 atoms were used to determine the rigid body motion of the molecule.[37] The results are given in Table VII.

Table VII. Rigid-Body Motion Parameters[a]

L ($\sigma(L)$), deg^2	19 (2)	3 (2)	−5 (2)
		24 (3)	−2 (2)
			20 (1)

Principal axes	Eigenvalue	Direction cosines × 10^3		
L, deg^2	27	−520	−704	483
	21	−395	700	595
	15	−757	120	−642
Reduced T, (Å)^2 × 10^4	336	732	58	−679
	256	−397	847	354
	244	554	529	643
Reduced S, Å rad × 10^4	19	−786	−10	−618
	3	−384	−776	501
	23	−484	631	606

Symmetrizing origin, Å	ζ_1 =	0.056
	ζ_2 =	−0.198
	ζ_3 =	0.417

Coordinates of displaced axes, Å	$^2\zeta_1$ =	0.02	$^1\zeta_2$ =	0.38
	$^3\zeta_1$ =	0.11	$^2\zeta_3$ =	0.46
	$^1\zeta_2$ =	−0.22	$^3\zeta_2$ =	−0.16

Effective screw translations, Å, parallel to	$L1$ =	0.004
	$L2$ =	−0.028
	$L3$ =	0.028

[a] The notation is that of Schomaker and Trueblood.[37] Their reference axes are a, b, c^*. The reduced T and S are those corresponding to eq 20 and 12 of ref 37. The positions of the symmetrizing origin and the axis displacements are relative to the center of mass and measured parallel to the principal libration axes.

The fit of a rigid-body model to the thermal parameters can be gauged from the rms $\Delta\mathbf{U}(I, J)$ of 0.0030 Å^2, where $\Delta\mathbf{U}(I, J)$ is the difference between the individual atomic displacement tensors $\mathbf{U}(I, J)$ and those calculated from the rigid-body parameters. In every case but one, the individual $\Delta\mathbf{U}(I, J)$'s are less than 1.5 times the estimated standard deviation of $\mathbf{U}(I, J)$, so the rigid-body approximation seems to be within the precision of the data.

It is of interest to examine the relative magnitudes of the mean-square amplitudes of rotational displacement about their principal axes and the relationship of these axes to the principal inertial axis system. In a recent paper, it was emphasized that the principal axis of libration for TCNQ and a number of its derivatives is always nearly along the axis of minimum inertia, and this was taken to mean that the pattern of lattice modes may be less sensitive to the details of the intermolecular potential than has been previously believed.[38] Some qualitative discussion of the anisotropy of the intermolecular potential and, in particular, a discussion of the attractive and repulsive forces which act upon free rotational motion of the molecule about its inertial axes should be included to fully substantiate an argument of this type. TCNQ represents the case of a molecule with particularly large inertial anisotropy so that it might be expected that the intermolecular potential is less important in defining molecular librations. It is of interest, therefore, to examine the librations of a molecule such as TCEO which does not have a large inertial anisotropy.

As discussed above, at the equilibrium configuration there are a number of nitrogen–carbon contacts of less than 3.2 Å. A free rotational motion of the TCEO molecule in the crystal will be interrupted mainly by the attractive forces between the nitrogen lone pairs and the electron-deficient group of three carbon atoms. The principal inertial axes are apparent from the symmetry of the molecule. The moment of inertia is largest about the molecular twofold axis. The minimum inertial axis is perpendicular to the plane of the ring through the center of gravity and has a moment of inertia only 45% less than that of the maximum inertial axis. The inertia about the third axis is very similar in magnitude to that about the minimum inertial axis, being about 10% larger. The inertia ellipsoid in the case of TCEO is seen to be fairly isotropic especially for any axis in the plane perpendicular to the axis of twofold symmetry through the center of gravity of the molecule. In Table VII we present the relevent information concerning the rigid-body motion. The translational motion is nearly isotropic, and the principal axes lie near to the principal molecular axes. The librational motion exhibits only a slight anisotropy as a result of no large directional differences in the inertia and the similar way in which each nitrogen contacts adjacent molecules. Of interest is the fact that the principal axis of libration bears no special relation to the molecular axis of minimum inertia. Thus, when the inertial anisotropy is not severe, the largest molecular librations will not in general be around the minimum axis of inertia even when the intermolecular potential is fairly isotropic. That is, the molecular librations of most molecules can be expected to be quite sensitive to the details of the intermolecular potential.

Since the translational and screw tensors T and S vary with the choice of origin, the reduced quantities which are origin independent are given.[37] The mutual displacements of the librational axes in the nonintersecting axis description are also given. The displacements of these axes from one another ($^I\zeta_k - {}^J\zeta_k$) (for axes I and J) are seen to be rather small, amounting in every case to less than 0.1 Å.

Acknowledgments. We wish to thank Dr. L. Heaton for his help in the collection of the neutron diffraction data which was obtained under the auspices of the Atomic Energy Commission.

(37) V. Schomaker and K. N. Trueblood, *Acta Crystallogr., Sect. B*, 24, 63 (1968).

(38) K. N. Trueblood, "Precise Diffraction Studies of Organic Crystal Structures, Contribution to 2nd Materials Research Symposium, 'Molecular' Dynamics and Structure of Solids," Natural Bureau of Standards, 1967.